Supporting Information: Measurement of hetero-nuclear distances using a symmetry-based pulse sequence in solid-state NMR

Lei Chen,[a] Qiang Wang,[a,b,c] Bingwen Hu,[b,d] Olivier Lafon,[b] Julien Trébosc,[b] Feng Deng,[a*] Jean-Paul Amoureux,[b*]

[a] *State Key Laboratory of Magnetic Resonance and Atomic and Molecular Physics, Wuhan Center for Magnetic Resonance, Wuhan Institute of Physics and Mathematics, the Chinese Academy of Sciences, Wuhan 430071, China*

[b] *Unit of Catalysis and Chemistry of Solids - UMR CNRS 8181, Université de Lille 1, 59652 Villeneuve d'Ascq cedex, Lille, France*

[c] *Graduate School of the Chinese Academy of Sciences, Beijing, China*

d Present address: Shanghai Key Laboratory of Magnetic Resonance, East China Normal University, 3663 Northern Zhongshan Road, Shanghai 200062, China

[*] Corresponding authors.
dengf@wipm.ac.cn, Tel: (86) 27-87198820, Fax: (86) 27-87199291
jean-paul.amoureux@univ-lille1.fr, Tel: (33)3.20.43.41.43, Fax: (33)3.20.43.68.14

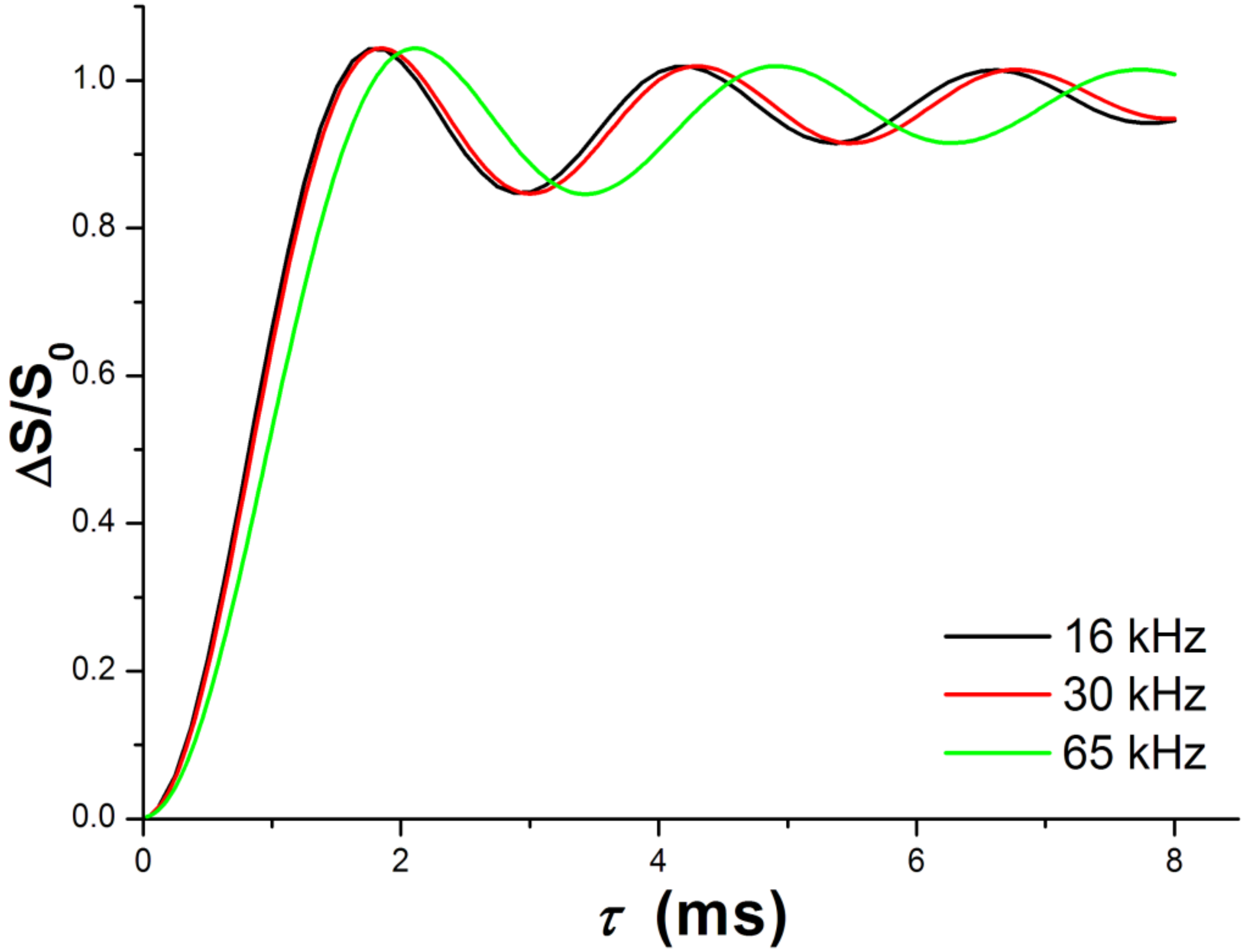

Fig.S1. Simulated signal fraction $\Delta S/S_0$ of REDOR as function of the recoupling time τ. The curves were calculated at different MAS frequencies, ν_R = 16, 30 and 65 kHz for ^{13}C-^{15}N spin system with $b_{13C\text{-}15N}/(2\pi)$ = -937 Hz. The anisotropic chemical de-shielding constant, δ_{aniso} (^{13}C), is equal to 8 kHz and the asymmetry parameter is η_{CSA} (^{13}C) = 0.5. The ^{15}N CSA was disregarded. The length of all REDOR π-pulses was equal to 6.25 μs, i.e. a nutation frequency ν_1 (^{13}C) = 80 kHz. The REDOR scheme is applied to the observed ^{13}C nuclei. The central π-pulse on the ^{15}N channel is ideal.

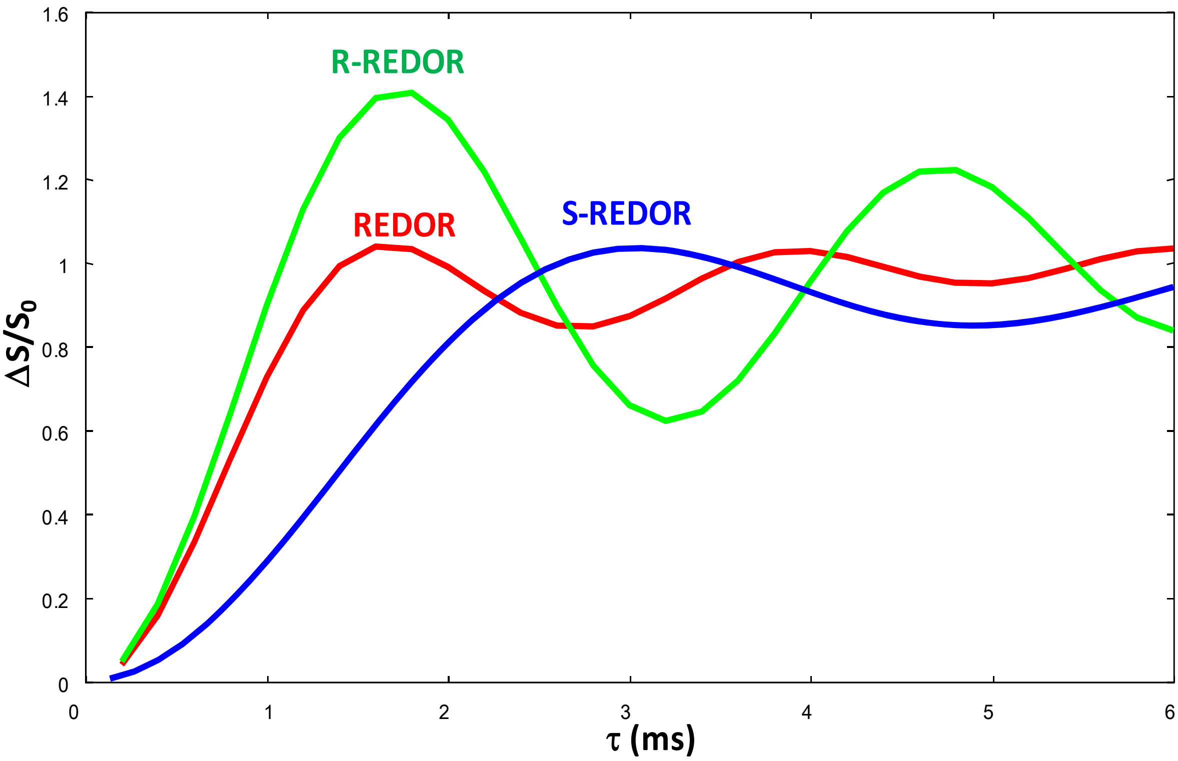

Fig.S2. Simulated signal fraction $\Delta S/S_0$ of REDOR, S-REDOR and R-REDOR as function of recoupling time τ. The curves were calculated at ν_R = 16 kHz for ^{13}C-^{15}N spin system with $b_{13C\text{-}15N}/(2\pi)$ = -1 kHz. The z principal axis of ^{13}C CSA tensor is aligned along the ^{13}C-^{15}N inter-nuclear direction and the anisotropic chemical de-shielding constant, δ_{aniso} (^{13}C), is equal to 8 kHz and η_{CSA} (^{13}C) = 0.5. The ^{15}N CSA was disregarded. REDOR sequence only uses perfect π-pulses. The nutation frequencies of $SR4_1^2$ and R^3 (n = 1) recoupling were fixed to their nominal values, $\nu_1 = 2\nu_R$ and $\nu_1 = \nu_R$. The REDOR, $SR4_1^2$ and R^3 (n = 1) schemes are applied to the observed nuclei, S = ^{13}C. The central π-pulses in S-REDOR sequence are infinitely short.

(a)

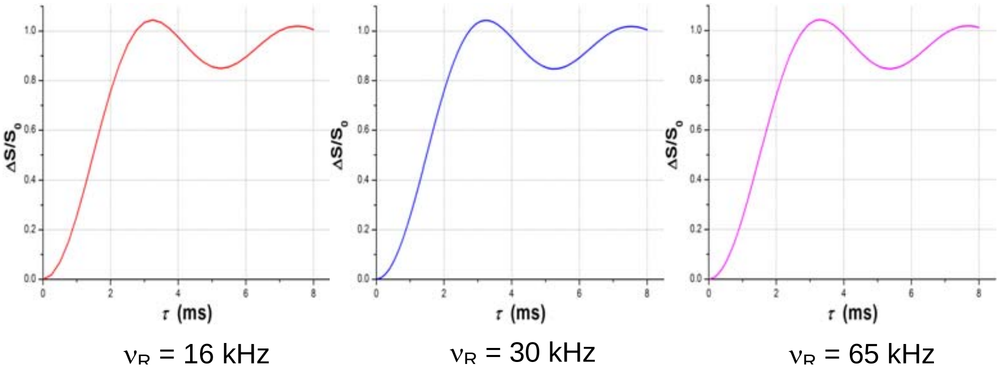

(b)

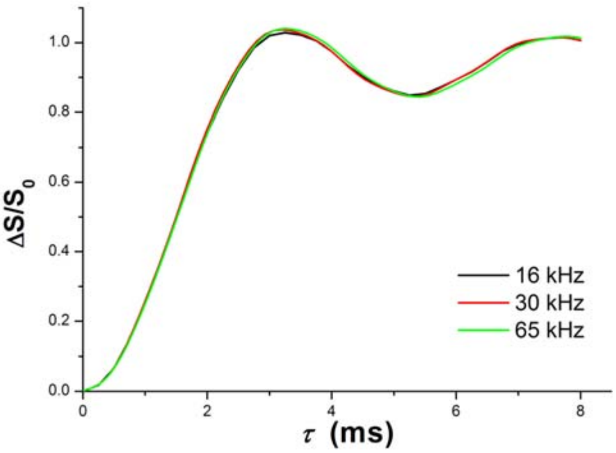

Fig.S3. Simulated signal fraction $\Delta S/S_0$ of S-REDOR as function of recoupling time τ. The curves were calculated at different MAS frequencies, ν_R = 16, 30 and 65 kHz for ^{13}C-^{15}N spin system with $b_{13C\text{-}15N}/(2\pi)$ = -937 Hz. The anisotropic chemical de-shielding constant, δ_{aniso} (^{13}C), is equal to 8 kHz and the asymmetry parameter is η_{CSA} (^{13}C) = 0.5. The ^{15}N CSA was disregarded. The nutation frequency of $SR4_1^2$ recoupling was fixed to its nominal value, $\nu_1 = 2\nu_R$. The recoupling was applied either (a) to the observed $S = {}^{13}C$ or (b) to the non-observed $I = {}^{15}N$ channels. The central π-pulses in S-REDOR sequence are ideal.

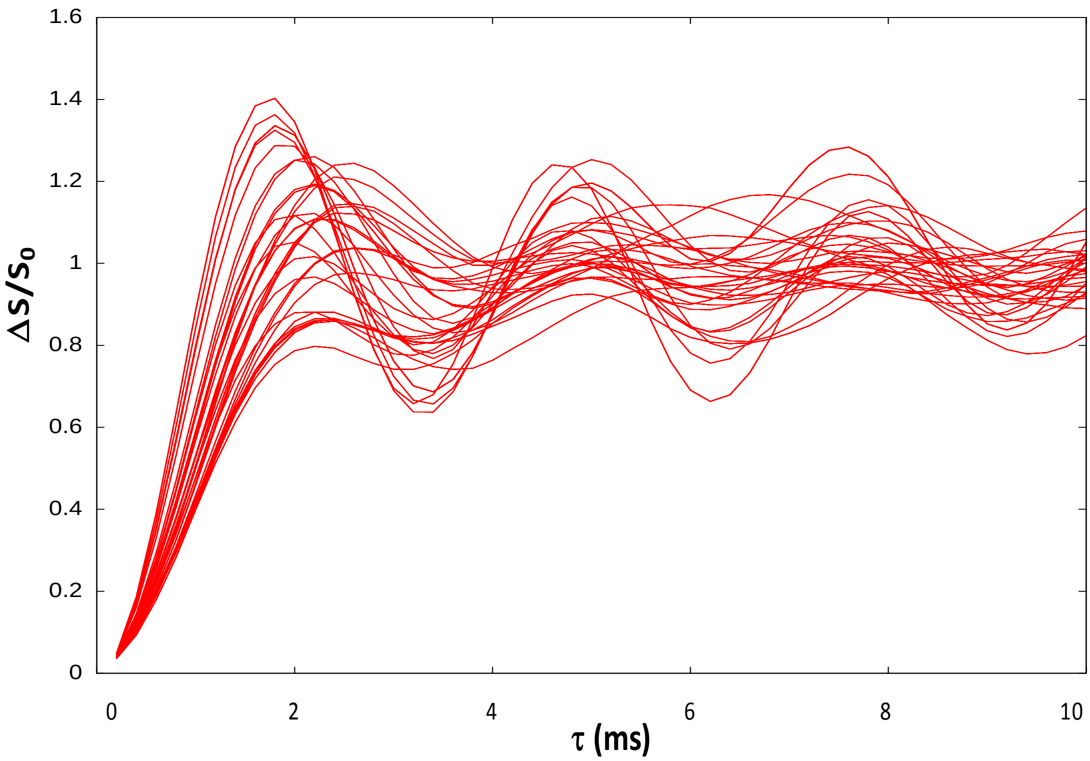

Fig.S4. Simulated signal fraction $\Delta S/S_0$ of R-REDOR as function of recoupling time τ using 30 uniformly-distributed orientations of ^{13}C CSA. The curves were calculated at ν_R = 30 kHz for ^{13}C-^{15}N spin system with $b_{13C\text{-}15N}/(2\pi)$ = -1 kHz. The R^3 recoupling is applied to the observed nucleus, S = ^{13}C. δ_{aniso} (^{13}C) = 8 kHz and η_{CSA} (^{13}C) = 0.5. The other simulation parameters are identical to those of Fig.S2.

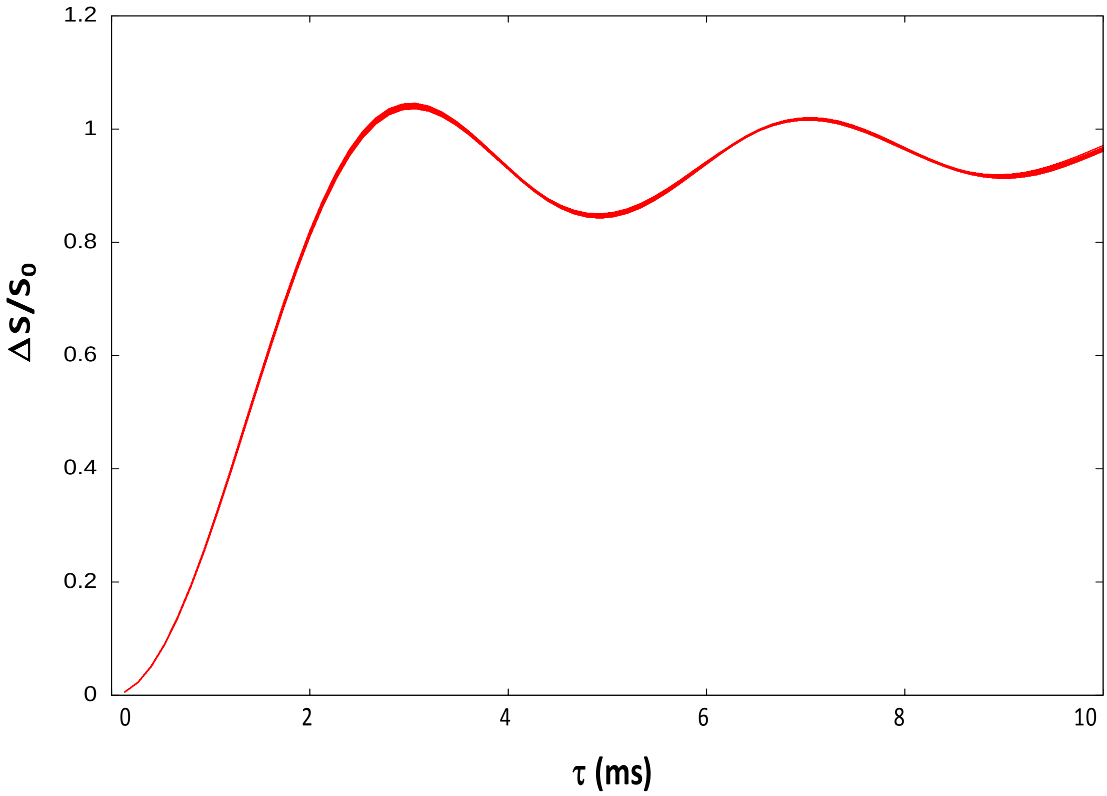

Fig.S5. Simulated signal fraction $\Delta S/S_0$ of S-REDOR as function of recoupling time τ using 30 uniformly-distributed orientations of ^{13}C CSA. The curves were calculated at ν_R = 30 kHz for ^{13}C-^{15}N spin system with $b_{13C\text{-}15N}/(2\pi)$ = -1 Hz. The $SR4_1^2$ recoupling is applied to the observed nucleus, S = ^{13}C. δ_{aniso} (^{13}C) = 8 kHz and η_{CSA} (^{13}C) = 0.5. The other simulation parameters are identical to those of Fig.S2.

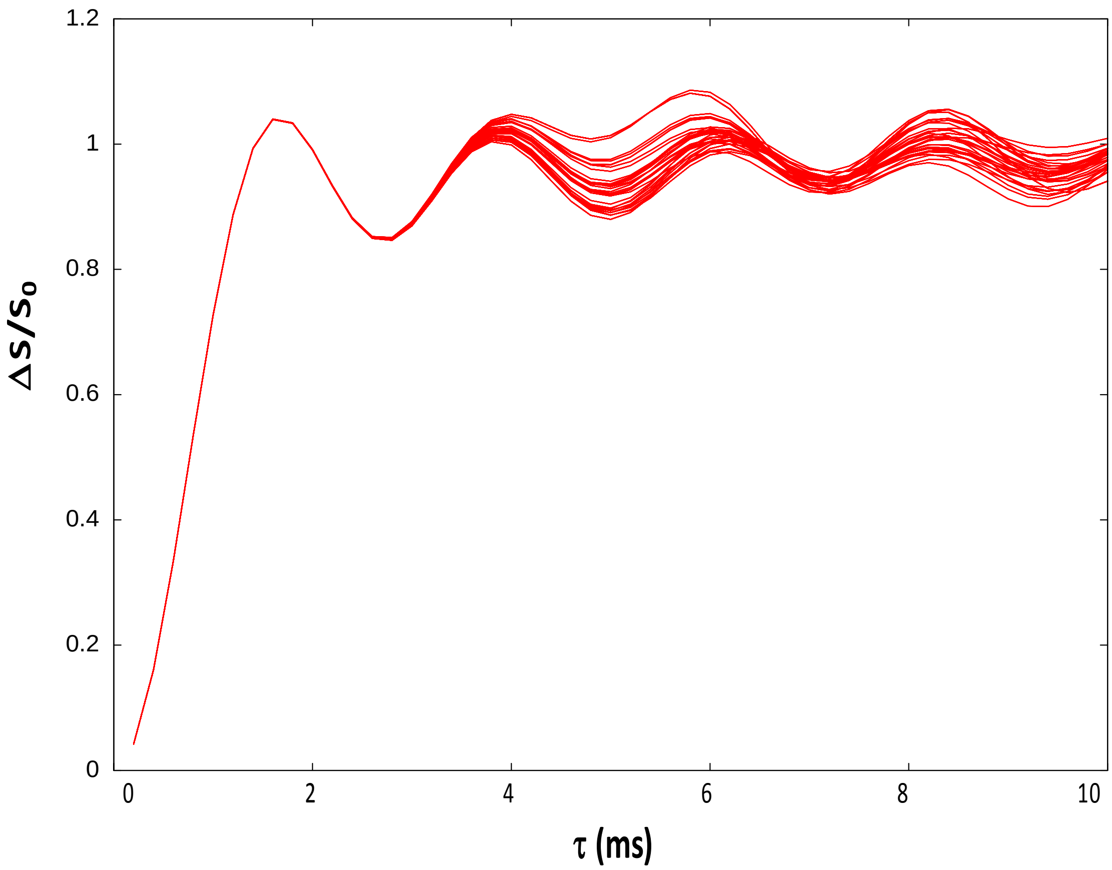

Fig.S6 Simulated signal fraction $\Delta S/S_0$ of REDOR as function of recoupling time τ using 30 uniformly-distributed orientations of ^{13}C CSA. The curves were calculated at ν_R = 30 kHz for ^{13}C-^{15}N spin system with $b_{13C\text{-}15N}/(2\pi)$ = -1 kHz. The REDOR recoupling is applied to the observed nucleus, S = ^{13}C. δ_{aniso} (^{13}C) = 8 kHz and η_{CSA} (^{13}C) = 0.5. The other simulation parameters are identical to those of Fig.S2.

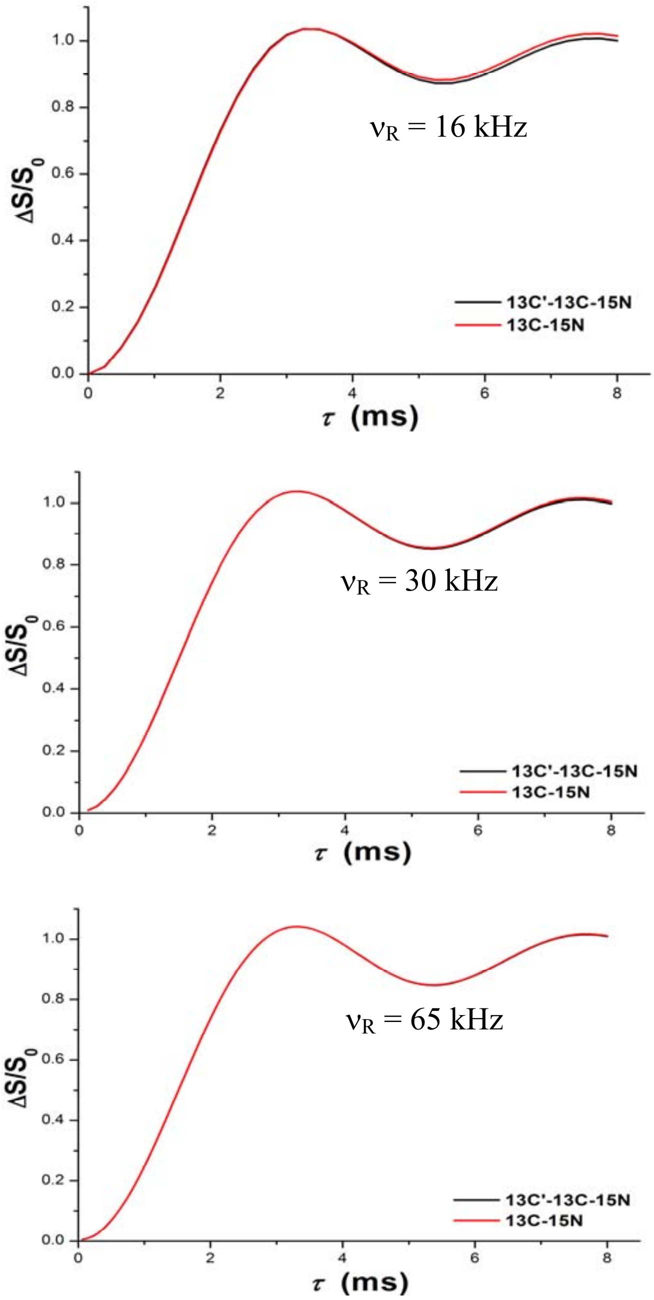

Fig.S7 Simulated signal fraction $\Delta S/S_0$ of S-REDOR as function of recoupling time τ. The red and black curves were calculated for ^{13}C-^{15}N two-spin and ^{13}C'-^{13}C-^{15}N three-spin systems at ν_R = 16, 30 or 65 kHz. For the two-spin system, the dipolar coupling constant is $b_{13C\text{-}15N}/(2\pi)$ = -937 Hz, while for the three-spin system, the additional dipolar coupling constant is $b_{13C\text{-}13C'}/(2\pi)$ = -2 kHz. The three nuclei are aligned in the ^{13}C'-^{13}C-^{15}N system and the dipolar coupling between ^{13}C' and ^{15}N is neglected. The anisotropic chemical de-shielding constant, δ_{aniso} (^{13}C) = 8 kHz and η_{CSA} (^{13}C) = 0.5. The ^{13}C' and ^{15}N CSA are disregarded. The nutation frequency of $SR4_1^2$ recoupling is fixed to its nominal value, $\nu_1 = 2\nu_R$. The recoupling is applied to the observed nuclei, S = ^{13}C. The central π pulses in S-REDOR sequence are infinitely short. The Euler angles defining the different interactions are as follows: $\Omega_{PC}^{13C-15N} = \{10^\circ, 20^\circ, 30^\circ\}$, $\Omega_{PC}^{13C-13C'} = \{40^\circ, 60^\circ, 80^\circ\}$, $\Omega_{PC}^{CSA,13C} = \{50^\circ, 20^\circ, 10^\circ\}$.

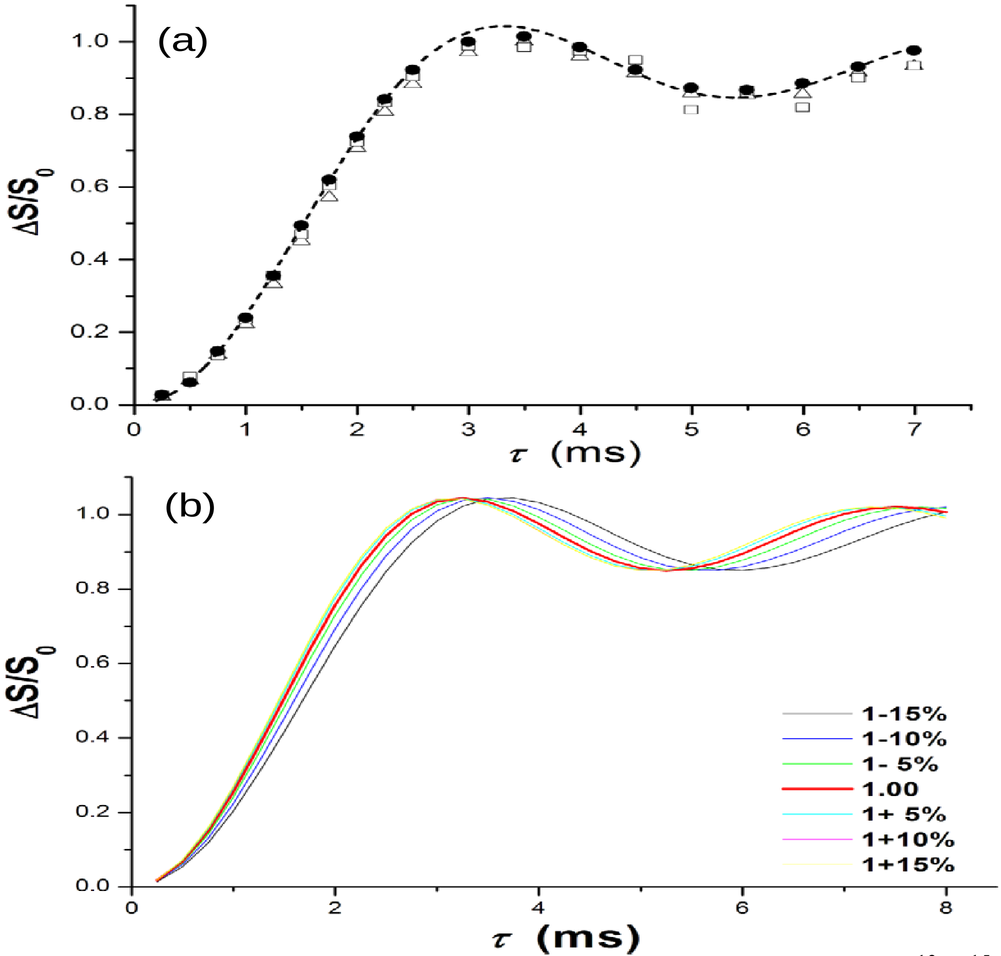

Fig.S8. Effect of rf field inhomogeneity on the signal fraction curves of ^{13}C-^{15}N S-REDOR experiment at ν_R = 16 kHz. The $SR4_1^2$ scheme is sent on the ^{13}C-observed channel. (a) Experimental signal fraction as function of τ for [2-^{13}C,^{15}N]-glycine with a full rotor sample. The rf field strength for the $SR4_1^2$ scheme is equal to its nominal value, ν_1 (^{13}C) = 32 kHz, (●) or 10% weaker (□), and 10% larger (△) than 32 kHz. The central π pulse nutation frequencies were $\nu_{1,\pi}$ (^{13}C) = 50 kHz , $\nu_{1,\pi}$ (^{15}N) = 45 kHz. The best fit curve according to Eq.11 for nominal rf field value is shown as a dashed line. The fitted ^{13}C$_\alpha$–^{15}N dipolar coupling constants are equal to $|b_{13C\alpha-15N}|/(2\pi)$ = 905, 873, and 882 Hz for the nominal, 10% weaker, and 10% larger rf values. (b) Simulated signal fraction curves for a set of rf nutation frequencies for the $SR4_1^2$ scheme in the range ν_1 (^{13}C) = 27.2-36.8 kHz. The central ^{13}C and ^{15}N π-pulses are infinitely short. The ^{13}C-^{15}N spin system is characterized by $b_{13C\text{-}15N}/(2\pi)$ = -937 Hz (corresponding to $D_{13C\text{-}15N}$ = 1.48 Å), δ_{aniso} (^{13}C) = 8 kHz and η_{CSA} (^{13}C) = 0.5. The ^{15}N CSA was disregarded. The fitted dipolar constants using Eq.11 for these curves simulated with different rf fields are: 823 Hz (1-15%), 866 Hz (1-10%), 902 Hz (1-5%), 932 Hz (1.00), 949 Hz (1+5%), 959 Hz (1+10%), 959 Hz (1+15%). The corresponding ^{13}C-^{15}N distances are equal to: 1.55, 1.52, 1.50, 1.49, 1.48, 1.47, and 1.47 Å.

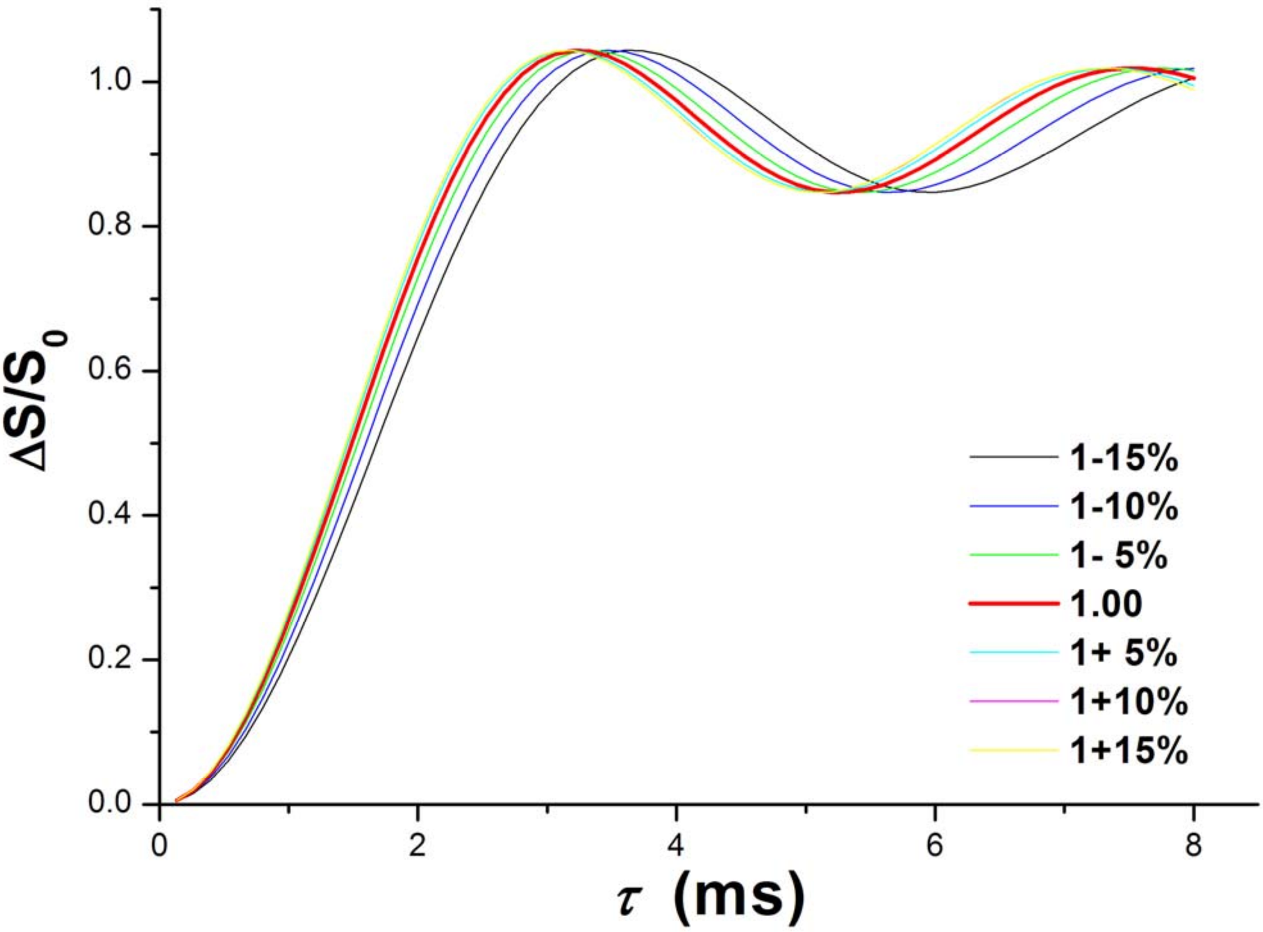

Fig.S9 Simulated signal fraction $\Delta S/S_0$ of S-REDOR as function of recoupling time τ at ν_R = 30 kHz using nominal rf frequency of $2\nu_R$ = 60 kHz as well as rf nutation frequencies 15%, 10% and 5% weaker or stronger than 60 kHz. The other simulation parameters are identical to those of Fig.S8. $b_{13C\text{-}15N}/(2\pi)$ = -937 Hz, δ_{aniso} (^{13}C) = 8 kHz and η_{CSA} (^{13}C) = 0.5. The ^{15}N CSA was disregarded. The central π pulses in S-REDOR sequence are infinitely short.

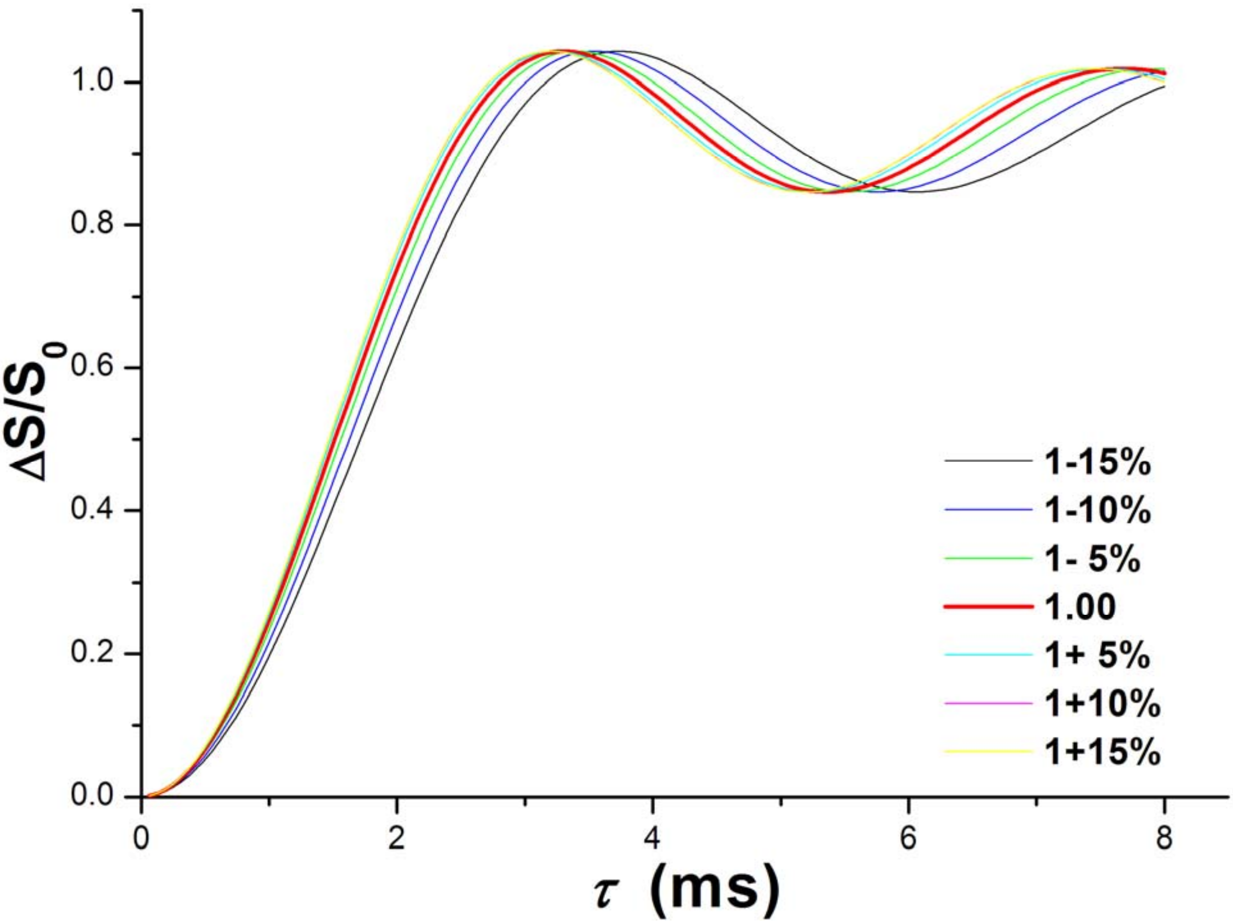

Fig.S10. Simulated signal fraction $\Delta S/S_0$ of S-REDOR as function of recoupling time τ at ν_R = 65 kHz using nominal rf frequency of $2\nu_R$ = 130 kHz as well as rf nutation frequencies 15%, 10% and 5% weaker or stronger than 130 kHz. The other simulation parameters are identical to those of Fig.S8. $b_{13C\text{-}15N}/(2\pi)$ = -937 Hz, δ_{aniso} (^{13}C) = 8 kHz and η_{CSA} (^{13}C) = 0.5. The ^{15}N CSA was disregarded. The central π pulses in S-REDOR sequence are infinitely short.

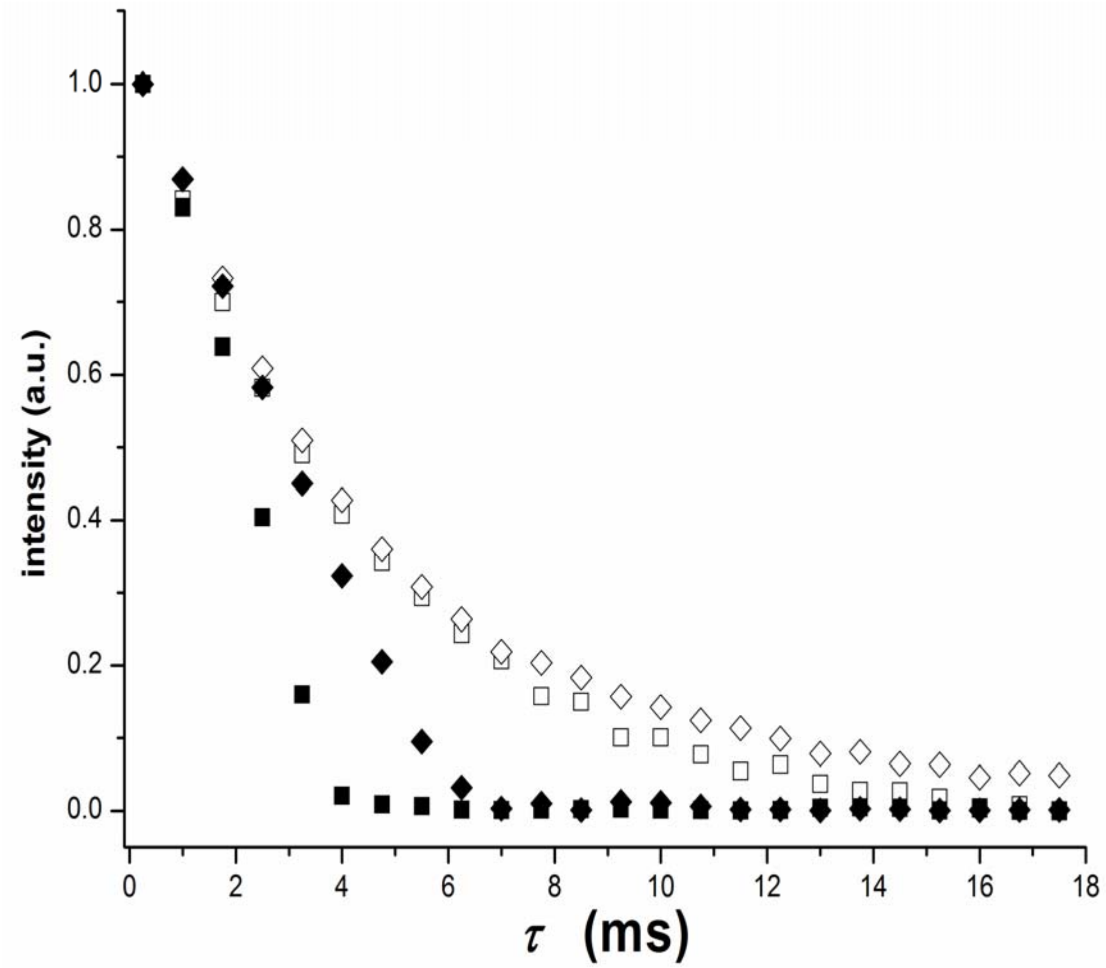

Fig.S11. Experimental ^{13}C-^{15}N S-REDOR S_0 signal for [2-^{13}C,^{15}N]-glycine. Experiments were performed at ν_R = 16 kHz (□,◇) and 15.980 kHz (■,◆). The nutation frequency of the central ^{13}C π-pulses was $\nu_{1,\pi}(^{13}C)$ = 50 kHz. The $SR4_1^2$ recoupling sequence, with nutation frequency of 32 kHz, was applied to the ^{13}C-observed (□,■) or the ^{15}N-non-observed (◇,◆) channel.

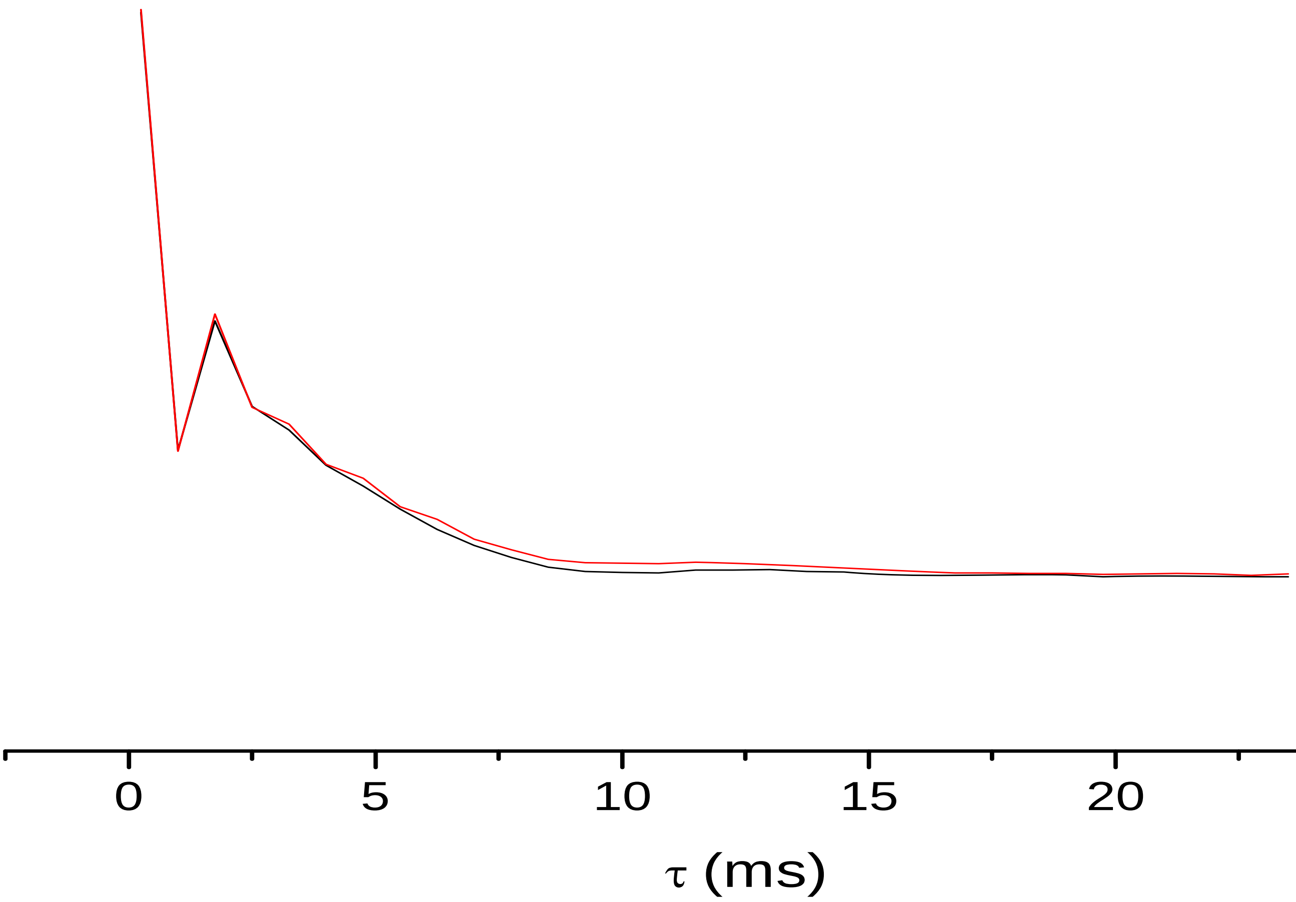

Fig.S12. Experimental ^{13}C-^{15}N R-REDOR S_0 signal for [2-^{13}C,^{15}N]-glycine. Experiments were performed at ν_R = 16 kHz (black) and 15.980 kHz (red). The nutation frequency of the central ^{13}C π-pulse was $\nu_{1,\pi}$ (^{13}C) = 55 kHz. The R^3 (n = 1) recoupling sequence, with nutation frequency of 16 kHz, was applied to the ^{13}C-observed channel.

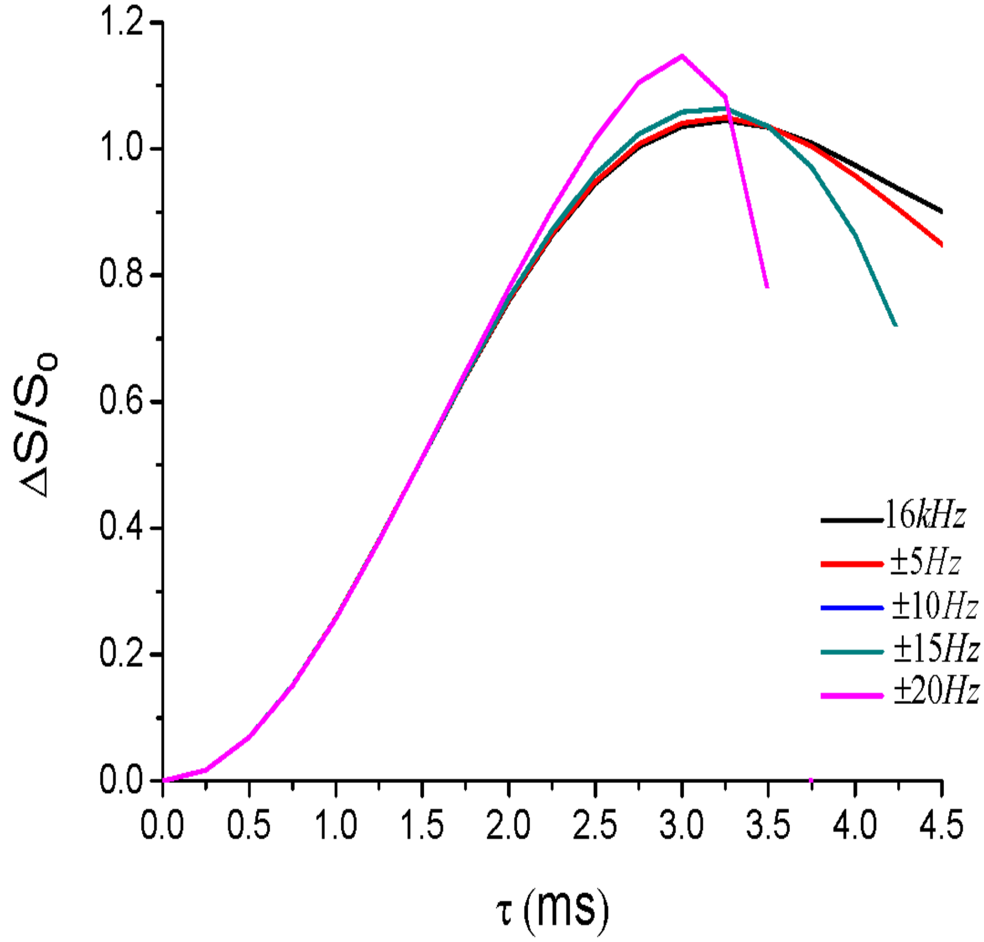

Fig.S13. Simulated ^{13}C-^{15}N S-REDOR signal fraction versus the recoupling time τ. The curves were calculated at different MAS frequencies in the range 15.980-16.020 kHz in steps of 5 Hz. The $SR4_1^2$ scheme was applied to the ^{13}C-observed channel and the recoupling nutation frequency was 32 kHz. The central ^{13}C and ^{15}N π pulses are infinitely short. The ^{13}C-^{15}N spin system is characterized by $b_{13C\text{-}15N}/(2\pi)$ = -937 Hz, δ_{aniso} (^{13}C) = 8 kHz and η_{CSA} (^{13}C) = 0.5. The ^{15}N CSA was disregarded. It must be noted that the simulation of these curves requires the full calculation of S and S_0. As an example S_0 is no more equal to 1 (see Fig.S11) as in rotor synchronized experiments. This leads to quite time-consuming calculation of $\Delta S/S_0$ fractions.

Validity of Eq.9.

For the sake of concision, in the following we use the notations (θ and ξ are real numbers):

$$I_{m=2} = \int_0^{2\pi} \mathrm{d}\gamma \int_0^{\pi} \mathrm{d}\beta \sin[\beta] \cos\{\theta \sin^2[\beta] \cos[2(\gamma+\xi)]\} \tag{A1}$$

and

$$I_{m=1} = \int_0^{2\pi} \mathrm{d}\gamma \int_0^{\pi} \mathrm{d}\beta \sin[\beta] \cos\{\theta \sin[2\beta] \cos[\gamma]\} \tag{A2}$$

1) We start by simplifying $I_{m=2}$. As the function

$$f(\beta,\gamma,\theta,\xi) = \sin[\beta] \cos\{\theta \sin^2[\beta] \cos[2(\gamma+\xi)]\} \tag{A3}$$

is periodic with respect to γ, with period π, the integral of $f(\beta,\gamma,\theta,\xi)$ with respect to γ over an interval of length 2π does not depend on the position of the interval and thus by setting $\gamma' = \gamma + \xi$, one obtains:

$$I_{m=2} = \int_{2\xi}^{2\pi+2\xi} \mathrm{d}\gamma \int_0^{\pi} \mathrm{d}\beta \sin[\beta] \cos\{\theta \sin^2[\beta] \cos[2\gamma]\} = \int_0^{2\pi} \mathrm{d}\gamma \int_0^{\pi} \mathrm{d}\beta \sin[\beta] \cos\{\theta \sin^2[\beta] \cos[2\gamma]\}. \tag{A4}$$

Eq.A4 can be calculated with zero-order Bessel function of the first kind, J_0,[1,2]

$$I_{m=2} = 2\pi \int_0^{\pi} \mathrm{d}\beta \sin[\beta] J_0\{|\theta| \sin^2[\beta]\}. \tag{A5}$$

By using $x = \cos[\beta]$, one obtains:

$$I_{m=2} = 2\pi \int_{-1}^{1} \mathrm{d}x J_0\{|\theta|(1-x^2)\}. \tag{A6}$$

2) We now simplify $I_{m=1}$, which may be reduced to a single integral over β by using J_0 function:

$$I_{m=1} = 2\pi \int_0^{\pi} \mathrm{d}\beta \sin[\beta] J_0\{|\theta \sin[2\beta]|\} \tag{A7}$$

We assume a change of variable $\phi = \pi/2 - \beta$ and rewrite $I_{m=1}$ as

$$I_{m=1} = 2\pi \int_{-3\pi/4}^{\pi/4} \mathrm{d}\phi \frac{\cos[\phi]}{\sqrt{2}} J_0\{|\theta \cos[2\phi]|\} - 2\pi \int_{-3\pi/4}^{\pi/4} \mathrm{d}\phi \frac{\sin[\phi]}{\sqrt{2}} J_0\{|\theta \cos[2\phi]|\}. \tag{A8}$$

The substitution $u = \sqrt{2}\cos[\phi]$ and $v = \sqrt{2}\sin[\phi]$ in the first and second integrals of Eq.A8 yields

$$I_{m=1} = \pi \int_{-1}^{1} \mathrm{d}u J_0\{|\theta|\,|1-u^2|\} + \pi \int_{-1}^{1} \mathrm{d}v J_0\{|\theta|\,|v^2-1|\} \tag{A9}$$

As $(u^2,v^2) \in [0,1]^2$, we have $|1-u^2| = 1-u^2$ and $|v^2-1| = 1-v^2$. Both integrals in Eq.A9 are thus identical, and hence we find $I_{m=1} = I_{m=2}$, which proves the validity of Eq.9.

[1] G.B. Harfken, H.J. Weber, Mathematical methods for physicists, 6th Edition, Elsevier Academic Press, Burlington, 2005.
[2] G.N. Watson, Theory of Bessel functions, Cambridge University Press, Cambdrige, 1944.